INTERNATIONAL JOURNAL OF CONSERVATION SCIENCE

ISSN: 2067-533X Volume 7, Issue 3, July-September 2016: 627-646 www.ijcs.uaic.ro

THE LONG TERM PRESERVATION OF LATE JURASSIC SANDSTONE DINOSSAUR FOOTPRINTS IN A MUSEUM ENVIRONMENT

Ana Sofia LEAL[1], Amélia DIONÍSIO[2*], Maria Amália SEQUEIRA BRAGA[2,3], Octávio MATEUS[4,5]

[1] Conservation and Restoration Department, Faculdade de Ciências e Tecnologia da Universidade Nova de Lisboa, 2829-516 Monte de Caparica
[2] Centro de Recursos Naturais e Ambiente (CERENA), Instituto Superior Técnico, Av. Rovisco Pais, 1049-001 Lisboa, Portugal
[3] Instituto de Ciências da Terra (ICT), Polo da Universidade do Minho, Departamento de Ciências da Terra, Campus de Gualtar, 4710-057 Braga, Portugal
[4] Museu da Lourinhã, Rua João Luís de Moura, 2530-157 Lourinhã, Portugal.
[5] Centro de Investigação em Ciência e Engenharia Geológica (CICEGe), Faculdade de Ciências e Tecnologia, FCT, Universidade Nova de Lisboa, 2829-516 Caparica, Portugal

Abstract

This study focuses on the assessment of the degradation processes occurring in three sandstone infills of fossilized Late Jurassic ornithopod tridactyl footprints, found in 2001 in a coastline cliff in Porto das Barcas (Lourinhã, Portugal) and exhibited in a museum display since 2004. These dinosaur footprints present nowadays severe decay phenomena compromising their physical integrity and leading gradually to their loss of value. The deterioration patterns were recorded, a map of their distribution was prepared and several samples were collected both in the dinosaur footprints and in the coastline cliff. Different analytical procedures were applied such as XRD, FTIR, FESEM and Ion Chromatography. A microclimatic survey was also performed and air temperature and relative humidity were measured during eight months both indoors and also outdoors. The decay patterns observed are a combination of intrinsic and extrinsic factors: the stone material, namely the swelling of clay minerals in the rock matrix(smectite and chlorite-smectite mixed-layer), the presence of salts (mainly chlorides), the application of past conservation treatments (poly(vinyl) acetate and epoxy resins) and the indoor thermohygrometric conditions (mainly non-stable hygrometric conditions) of the museum. This scientific knowledge is therefore essential to the sustainable preservation of this paleontological heritage.

Keywords: *Dinosaur footprints; Sandstone; Museum; Decay; Clay minerals; Salts; Past treatments; Environmental microclimate.*

Introduction

Dinosaur tracks and trace fossils are an extremely important branch of vertebrate ichnology. They provide valuable information that is very different from that furnished by body fossils, since they represent in situ evidence of the dynamic activity of dinosaurs in their lifetime [1]. Besides their scientific importance and ichnological significance, dinosaur tracks are also valuable for science popularization and to stimulate public interest for the preservation

* Corresponding author: amelia.dionisio@tecnico.ulisboa.pt,

of the paleontological heritage.

The deterioration of paleontological heritage can be a paradigm of a complex process influenced by the intrinsic properties of the materials like chemical composition, texture, porosity, etc., and by extrinsic factors, such as climatic conditions, damage induced by conservation procedures, vandalism and also by biological agents. So, it is necessary to understand the causes and mechanisms of decay in order to mitigate its effects and to intervene conscientiously. This scientific knowledge is therefore essential to the sustainable preservation of the paleontological heritage.

Nevertheless, little if any attempt appears to have been made to study the aging of dinosaur footprints after being prepared for exhibition in a museum environment. In fact several authors have been working on the systematic icnology [2], site reports [3, 4], locomotion and behaviour [5] and also on the conservation and preservation of tracksites [6].

The conservation of fossils and other cultural, scientific and natural heritage is often a preoccupation and concern of museum and collections curators. S.Y. Shelton [7] listed the most relevant agents of deterioration, namely physical neglect, thieves and vandals, fire, water, biodeterioration, air pollution, ultraviolet, visible and infrared radiation, temperature fluctuation and inappropriately high and low humidity.

In paleontology, the role of synthetic polymers glues, adhesives and consolidants is very important as they have been applied for a long time to bones and tracks. S.Y. Shelton and D.S. Chaney [8] provide an overview of their use in paleontology. Recent studies show that the low viscosity of an alkoxysilane consolidant (Conservare OH 100) was found to be particularly suited for the preparation of the fragile dinosaur fossils from Mongolia, increasing the strength of the bone, nevertheless it did not consolidate the surrounding sandstone [9]. Thus, the poor consolidation of the sandstone made it inefficient for track fossils in this material. J.L. Down and E. Kaminska [10] studied the degradation of cyanoacrylate adhesives in the presence and absence of fossil material showing that butyl cyanoacrylate degraded more slowly than ethyl cyanoacrylate, and that acidic fossil inhibits the degradation of cyanoacrylate while neutral or alkaline fossils increase the degradation.

Despite the numerous open-air visitable tracksites, susceptible to weathering, there is little research on the preservation and conservations of tracks [6, 11-13]. Even rarer are the studies concerning the degradation of tracks when exhibited in museum conditions. So, the present study aims to present a methodological study concerning the characterization of the degradation forms observed in three Late Jurassic sandstone dinosaur footprints exhibited in a museum environment [14], aiming to appraise the causes and mechanisms involved in their decay in order to identify conservation needs.

Materials and Methods

The geological setting

The Lourinhã Formation comprises distal deposits of a low relief alluvial fan sourced from the now submerged western margin of the Lusitanian Basin [15] (Fig. 1a). Fluvial channel sandstones, finer grained overbank deposits and floodplain mudstones are the primary components of the Lourinhã Formation, and deltaic deposits are present near the base of the succession [15, 16]. According to Myers et al. [17] the channel facies within the Lourinhã Formation consists of thick, fine to coarse-grained, lenticular sandstones that show little evidence of lateral continuity.

Three dinosaur footprints (ML557) were found on a coastline cliff in Lourinhã, Porto das Barcas, Lagido do Forno (coordinate 39° 14. 178'N, 9° 20. 397'W) on the 5th of June 2001 by Jesper Milàn and Octávio Mateus (Fig. 1b).

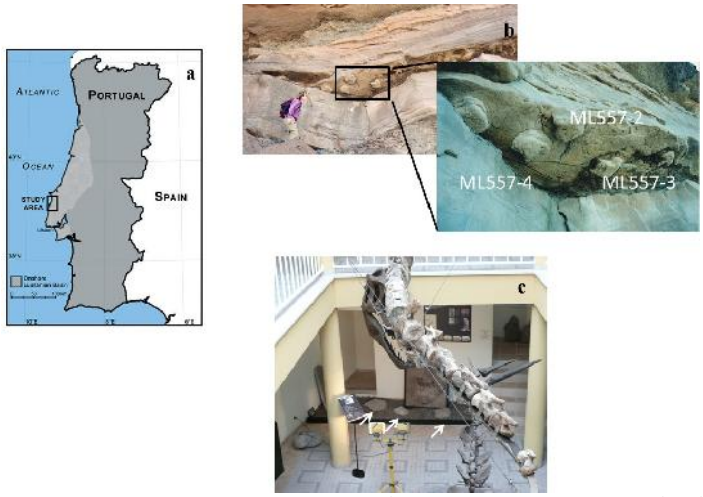

Fig. 1. Map of the studied area showing the onshore portion of the Lusitanian Basin (a), modified from Myers et al. [17]; localization of the dinosaur footprints in lenticular sandstone and samples references (b); location of the same dinosaur footprints and of the thermohygrometer in Lourinhã Museum (c).

This cliff of high slope presents sedimentary stratigraphic characteristics of a sandstone/siltstone of gray and red colors. Geologically the tracks are Late Jurassic in age, and were collected in the Lourinhã Formation, Praia Azul Member, of the Lusitanian Basin. These footprints correspond to three natural infills tridactyl tracks, possibly ascribed to ornithopod, a bipedal herbivore, resultant of a left foot movement, right and left. Footprints are 350-400mm wide and 330-360mm high with round fingers, which are elongated due to some degradation/erosion (Fig. 2). In 2001, the footprints were collected from the field, without showing any signs of deterioration. Thereafter they were subjected, in the laboratory of the Museum of Lourinhã to different conservation treatments (cleaning, consolidation and application of adhesives), that allowed them to be properly handled and exhibited in a museum display (Fig. 1c). No reference to the application in these footprints of a desalination treatment was found. The extent and rate of the dinosaur footprints' decay started sometime after being exhibited in a museum display.

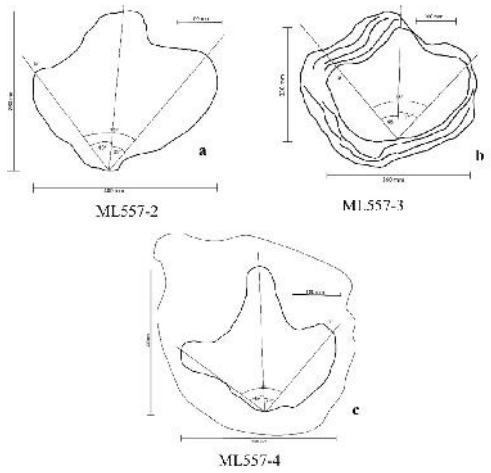

Fig. 2. Diagram drawing showing some measurements of the studied dinosaur footprints: ML557-2 (a); ML557-3 (b) and ML557-4 (c).

Condition survey: weathering forms, mapping and sampling

A detailed survey of decay phenomena was carried out on the three footprints in 2013. Deterioration and degradation patterns were classified and mapped. The terminology proposed by ICOMOS-ISCS was considered [18]. Detailed information was visually recorded on the type and the extent of the occurring damages. Deterioration and degradation patterns are the visible component of the decay processes that are operating onsite. They reflect the interaction between the stone intrinsic components and the environment or extrinsic factors [19].

Previously it was necessary to prepare drawn-to-scale planes of the footprints. Mapping is considered a non-destructive valuable element since it allows the quantitative evaluation of complete stone surfaces according to the type and the distribution of weathering forms. It records the current state of deterioration, gives information about the distribution of deterioration in an object and its extent and also easily locates the most deteriorated areas [20]. Mapping of degradation patterns and of any other kind of anomalies (Fig. 3) is a very powerful tool since it makes an important contribution to the rating of decay damage, decay prognosis, information on causes and processes of stone damage.

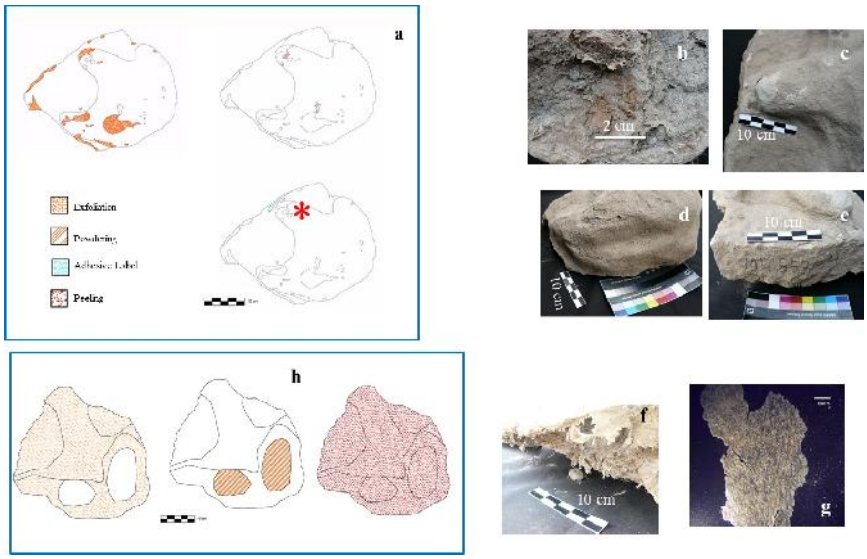

Fig. 3. Deterioration patterns observed in the footprint ML 557-4: Mapping of the front (a) and rear side (h); exfoliation and peeling (b); exfoliation (c); powdering (d); adhesive label (e); peeling (f) and detail of the peeling under stereomicroscope (g); * sampling site for µFTIR analysis.

The deterioration pattern maps (Fig. 3) contributed to the optimization of representative sampling for laboratory analysis and four samples (ML-557-2/3/4a/4b) were collected at different points and sides of these footprints (Fig. 4). Moreover two samples (PBA and PBB) from the coastline cliff were also collected nearby the place where those footprints were found.

Analytical Methods

Analytical methods for morphological, mineralogical and chemical studies were performed. The morphological and mineralogical study was carried out by stereomicroscope and X-ray diffraction (XRD). Scanning electron microscopy (SEM) associated with EDS microprobe (Energy Dispersive System) for chemical analysis, using X-rays and standard ZAF corrections that allow information on the elemental composition of the samples was used.

In order to evaluate the presence of clay minerals, with significant carbonate contents, it was necessary to have the calcite removed. The whole rock of the coastline cliff samples (PBA

and PBB), were submitted to acetic acid ≤0.3 molar, according to Moore and Reynolds [21]. After the carbonate has been dissolved and the samples well dispersed, the separation of the clay-sized fraction was accomplished [21, 22]. The XRD diffractograms from these two samples were obtained from powders (bulk sample) and from oriented mounts (<2µm). In the ML -557samples of the dinosaur footprints, the sample preparation techniques for clay minerals could not be applied due to the insufficient quantity of material for a suitable routine preparation. Therefore, the analysed grain size was <20µm. Nevertheless in the samples collected at the coastline cliff the procedure for clays study was followed [23, 24].

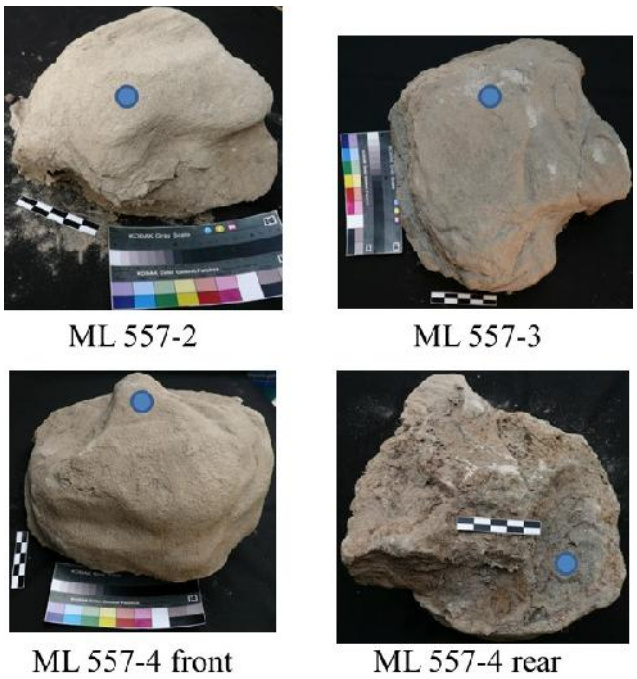

Fig. 4. Detail of the three footprints and deterioration patterns with indication of the sampling sites for Ion Chromatography.

Therefore, the XRD diffractograms for the mineralogical study were obtained from bulk rock (non-oriented preparations) and from oriented preparations of the <20µm. In what fine-fraction (<20µm) concerns, the bulk rock was submitted to wet sieving with a 20 µm sieve, because this fine-fraction includes clay and silt particles. For all samples from <2µm and <20µm fractions, the oriented mounts were subjected to the following treatments: air-dried, ethylene glycol (EG)-solvated and heated (490ºC). Regarding the semi-quantitative analyses of mineral phases in the bulk samples the peak-height intensities for diagnostic reflections were used [23]. Semi-quantitative analysis of clay minerals was deduced from the diagnostic peaks related to their first-order basal reflections at air-dried conditions or after EG solvation.

The XRD patterns were obtained using a Philips PW1710 diffractometer with CuKα radiation at 40kV and 30mA, with a 2 theta step size of 0.02º and a counting time of 1.25s. The diffractometer is provided with automatic divergence slit and graphite monochromator. The data obtained in this PW1710 (APD - 3.6j version) equipment were treated with X'Pert software – Philips Analytical.

SEM observations were carried out on rock fragment samples directly mounted on a sample stub and sputter coated with a thin gold/palladium film. They were examined on a JEOL JSM-7001F field emission scanning electron microscopy (FESEM) equipped with an Oxford X-

ray energy dispersive spectroscopy (EDS) detector. The study of the mineral phases associated to the semi-quantitative chemical microanalysis was performed by this technique.

Extraction of water-soluble fraction was performed by mixing a fixed amount of a stone sample (~2g) with 100 ml of Milli-Q water for two hours, followed by filtration. Water-soluble ions (Cl^-, SO_4^{2-} and NO_3^-) were analysed by Ion Chromatography (Dionex 2000i/SP). Moreover, the electrical conductivity (WTW Cond330i/set) and pH (WTW pH3110 Set A) of the solution were also determined.

The Fourier Transform InfraRed spectroscopic analysis (FTIR) was used to identify the nature of past treatments, their chemical characteristics and the formation of potential secondary products. Two samples were collected, one corresponding to the material that composes the peeling (Fig. 3g) and one to the film observed in the central part of the finger of the ML557-3 footprint (Fig. 3d). The FTIR spectra were obtained with a Nicolet Nexus equipped with a Continuum microscope, in transmittance mode using a diamond compression cell. The IR spectra were recorded for the $4000cm^{-1}$ to $650cm^{-1}$ region and a total of 128 scans recorded, as well as the resulting interferogram averaged. The mirror velocity was $1.8988cm{\cdot}s^{-1}$ with a resolution of $4cm^{-1}$. Acquisition and post-run processing were carried out using Nicolet "Omnic" software.

Climate Monitoring

It has long been accepted that thermal and moisture regimes within stonework exert a major influence upon patterns of salt movement and subsequently, upon the type and severity of salt-induced decay. Therefore, in order to make a quantitative description and analysis of the Lourinhã Museum indoor climate and to understand how building properties and outdoor climate variations influence the indoor climate, a microclimatic survey was performed. In what concerns the outdoor measurements, air temperature and relative humidity (RH) data were obtained from the meteorological observatory of Lourinhã (39º 13' 54" N, 9º 18' 29" W, see the Geological setting), provided by the Portuguese Sea and Atmosphere Institute (IPMA). The thermo-hygrometric conditions of the Museum have been monitored continuously from November 2, 2013 to March 6, 2014 and from May 24, 2014 to September 29, 2014. A Lascar Electronics Limited data logger (Model EL-USB-2) was used. The sensor was put near the dinosaur footprints (Fig. 1) and indoor air temperature and relative humidity data were logged every 30 minutes. This logger measures temperature from -35ºC to +80ºC with an accuracy of ±0.5ºC and RH from 0% to 100% with an accuracy ± 3%.

Results and Discussion

Mapping of the deterioration patterns

A detailed survey of decay phenomena was carried out on the three footprints and several deterioration patterns were identified. The observed deterioration patterns were classified in three main families: "Crack & Deformation", "Detachment" and "Discoloration and deposits" (Table 1 and Fig. 3 as an example of mapping).

The most relevant deterioration patterns were exfoliation (Fig. 3b and c), powdering (Fig. 3d) and soiling. A significant fracture was also observed in the dinosaur footprint ML 557-3. An attempt to glue the separate parts of the central finger was done and nowadays the material used shows signs of ageing (yellowing). Adhesive labels have also been identified in the dinosaur footprints ML 557-2 (Fig. 1 and Fig. 4) and ML557-4 (Fig. 3e and Fig. 4). Moreover the application of conservation treatments in the past seems to be no really effective solutions to preserve and protect these paleontological materials. Indeed severe partial detachment of a superficial layer having the aspect of a coating applied on the footprints is observed in Figure 3b and f. Under the stereomicroscope it was possible to observe that this layer had millimetric thickness (Fig. 3g), presented a yellowish colour, a glossy brightness, loss of elasticity and break easily. The documentation of deterioration patterns was done on scaled drawings (Fig. 3a and h). Besides the diversity of previously mentioned deterioration patterns,

their mapping allows to verify that the most representative degradation patterns taking up most of the footprint surfaces are: (i) surface loss by binding loosened sandstone grains, associated with (ii) detachment of previous applied treatments.

Table 1. Classification and description of the visually observed deterioration patterns (according to [18]) at the dinosaur footprints.

Family	Type/Subtype	Recording of the deterioration patterns
Crack & Deformation	Fissure/Fracture	Individual fissure, clearly visible by the naked eye, resulting from separation of one part from another/Crack that crosses completely the stone piece.
Detachment	Delamination/ Exfoliation	Physical separation into one or several layers following the stone laminae. The thickness and the shape of the layers are variable/ detachment of multiple thin stone layers (cm scale) that are sub-parallel to the stone surface (see Fig. 3a,b,c and h).
	Disintegration/ Powdering	Detachment of aggregates of grains from the substrate (See Fig. 3a, d and h).
	Peeling	Shedding, coming off, or partial detachment of a superficial layer (thickness: submillimetric to millimetric) having the aspect of a film or coating which has been applied on the stone surface. In this specific case separated, air-filled, raised hemispherical elevations on the film or coating is observed (see Fig. 3a and b).
Discoloration & Deposit	Soiling	Deposit of a very thin layer of exogenous particles (e.g. soot) giving a dirty appearance to the stone surface.
	Graffiti/ Adhesive label	Engraving, scratching, cutting or application of paint, ink or similar matter on the stone surface (see Fig. 3a and e).
	Film	Thin visible homogeneous coating layer that seems of organic nature.

Figure 3 clearly demonstrate the severe stone damage presented by the dinosaur footprints, leading to important material losses and even to the loss in value and significance.

The decay patterns identified in this paper mostly correspond to the general decay features associated to sandstone. In fact, B.J. Smith et al. [25] consider that sandstones are particularly prone to disruption by granular disintegration, contour scaling and multiple flaking. Moreover A.V. Turkington and T.R. Paradise [26] present a review of sandstone weathering research, particularly in the past 100 years, either in terms of description and classification of weathering/decay features, or either in terms of weathering/decay mechanisms and processes.

Morphological, mineralogical and chemical characterization

The stereomicroscope study showed an important textural feature observed on small rock fragments (ML-557-4c sample). Some blistered portions were observed and these rounded masses show a typical swelling-controlled morphology. This morphology was also observed in the remainder samples (ML-557-2; ML-557-3; ML-557-4a) of the dinosaur footprints. However, other subsamples for XRD analyses could not be obtained, due to the very small dimension of those rounded masses.

The bulk mineralogical composition (Table 2), obtained by XRD, comprises quartz, K-feldspar, plagioclase, micas, clay minerals, goethite, halite, calcite, strontianite, celestite, gypsum and chlorapatite. Calcite is the dominant mineral in all samples (estimated by XRD) and its amount varies between 30% and 20% (on average) in the coastline cliff and dinosaur footprints samples, respectively. Other mineral classes (carbonates, sulphates and phosphates) and subclasses (oxyhydroxides) are present in vestigial amounts (≤3%). Clay minerals are also present (≤2%) either in the coastline cliff samples or in the dinosaur footprints. Halite occurs in trace amounts (≤4%) in all samples, with the exception of the subsample ML-557-4c. It is in this sample that gypsum (3%) occurs. Besides, this sample is the unique one characterized by a particular morphology, when observed at stereomicroscope, as it was mentioned above.

Table 2. Mineralogical composition of the bulk rock samples estimated by XRD (%).

Sites	Samples	Q	F	P	Mi	CM	Go	Ha	Ca	Sr	Ce	Gy	Cap
Coastline cliff	PBA	21	17	21	15	2	1	6	15	-	tr	-	2
	PBB	18	18	11	2	1	tr	2	44	3	-	-	1
Dinosaur footprints	ML-557-2	32	23	20	5	2	1	2	14	tr	tr	n.d.	1
	ML-557-3	12	26	36	3	1	1	2	19	tr	tr	n.d.	tr
	ML-557-4a	26	22	22	7	2	1	2	16	-	-	n.d.	2
	ML-557-4b	27	14	19	8	1	1	tr	29	-	-	n.d.	1
	ML-557-4c	22	21	24	7	2	tr	-	21	tr	tr	3	-

Q - quartz; F – K feldspar; P - plagioclase; Mi - mica; CM - clay minerals; Go - goethite; Ha - halite; Ca - calcite; Sr - strontianite; Ce - celestite; Gy - gypsum; Cap - chlorapatite; tr - traces, n.d. - not determined.

Concerning bulk mineralogical composition, there are not large differences between the samples of the coastline cliff and dinosaur footprints. However, it must be noted that gypsum was not identified in the coastline cliff samples.

The semi-quantitative mineralogical composition of the fine fractions, obtained by XRD, is showed in Table 3, taking into account clay minerals and oxyhydroxides.

The < 2µm fraction collected from the coastline cliff (Table 3) comprises chlorite, illite, chlorite-smectite mixed-layer, smectite, kaolinite and goethite. In these samples (PBA and PBB), kaolinite is the dominant (81%) clay mineral. Table 3 also shows also the mineralogical composition of the <20µm fraction concerning dinosaur footprints samples (ML -557-2/3/4a/4b). All these samples are also dominated by kaolinite (84%, on average). Beside the fact that the amount of smectite and C-Sm mixed-layer are very small (≤7 % - Table 3), their presence can contribute to the typical swelling-controlled morphology in the dinosaur footprints samples. In spite of the studied fine fractions (<2µm and <20 µm) being different, they have a similar clay mineral composition in both sites (coastline cliff and dinosaur footprints).

Table 3. Mineralogical composition of the coastline cliff and dinosaur footprints samples estimated by XRD (%) in the <2µm and <20µm fractions.

Sites	Samples	Grain-size	Cl	Il	Cl-Sm	Sm	K	Go
Coastline cliff	PBA	< 2µm	2	10	2	5	81	tr
	PBB		2	10	2	4	81	1
Dinosaur footprints	ML-557-2	< 20µm	2	10	-	1	87	-
	ML-557-3		3	12	-	2	83	tr
	ML-557-4a		3	14	-	2	81	-
	ML-557-4b		2	9	-	1	84	4

Cl - chlorite; Il - illite; Cl-Smn - chlorite-smectite mixed-layer; Sm - smectite; K - kaolinite; Go - goethite; tr - trace.

Chlorite, illite, chlorite-smectite mixed-layer, smectite, kaolinite and goethite were the clays and oxyhydroxides minerals identified in the <2µm fraction. The XRD patterns (Fig. 5) kaolinite is characterized by intense and sharp peaks for the reflections 001 (7.19Å) and 002 (3.58Å). This behaviour suggests the high degree of order for kaolinite [27]. Smectite was identified by a basal spacing of 15.50Å in air-dried conditions with a basal spacing expanding to 16.62Å in EG-solvated conditions and collapsing to 10.05Å after heating at 490ºC. The

shape (broad bands) and intensity of the basal reflections indicate a poorly crystallized smectite. The basal and weak reflections centred at 14.24Å and 4.74Å in air-dried conditions, and at 14.35Å and 4.75Å after EG solvation, shifting to 12.6Å after heating at 490ºC, besides the presence of chlorite, suggest the occurrence of an mixed-layer chlorite-smectite. The shape of these small peaks associated to one broad band at near 31Å can be ascribed to that mixed-layer [21, 27]. Values for d_{001} of 10.07Å and d_{002} of 5.01Å indicate the presence of illite. Finally, and despite its small amount (Table 2 and Table 3), poorly crystallized goethite was identified by the broad peaks at ~4.20Å and 2.69Å (Fig. 5).

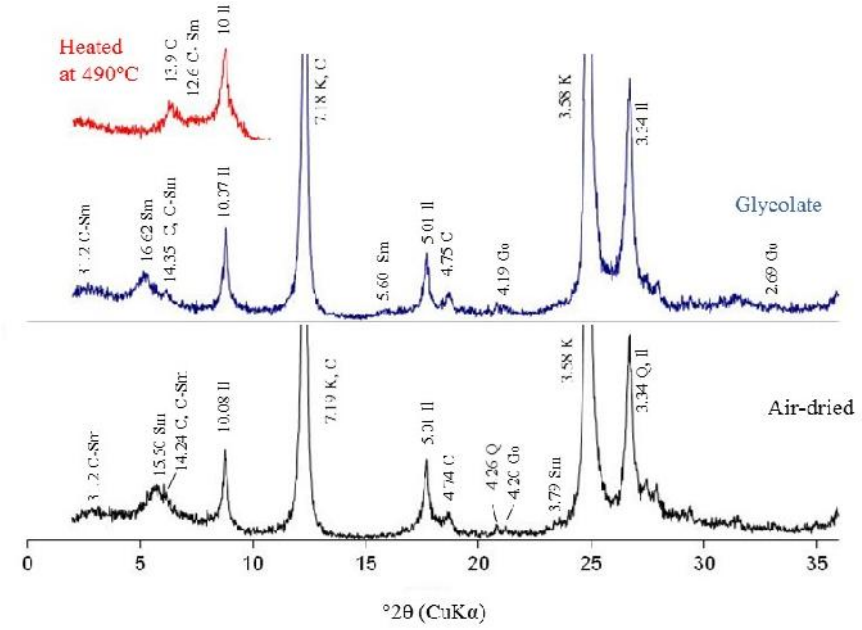

Fig. 5. XRD patterns from <2µm fraction of the coastline cliff sample (PBB) showing *d* values (Å) of Cl - chlorite; Il - illite; Cl-Sm - chlorite-smectite mixed-layer; Sm - smectite; K - kaolinite; Go - goethite.

FESEM and SEM-EDS studies performed on sandstone fragments, either on the coastline cliff or on the dinosaur footprints were used as complementary technique of the X-ray diffraction. This study is focused on the examination of the morphological and mineralogical features that may contribute to the knowledge of the degradation processes of the dinosaur tracks in Museum environment conditions.

The occurrence of a great number of etch pits characterize the calcite ($CaCO_3$) crystals (Fig. 6a, ML-557-3). Radiating crystal groups of celestite ($SrSO_4$) are associated to the calcite porosity (Fig. 6a and c). Chemical spectrum (Fig. 6b, ML- 557-3) shows the presence of elements from this sulphate mineral (Sr and S). Ba and Ca may be present in substitution for Sr in the structure of the celestite. Tuff of acicular crystals with slightly curved terminations can ascribe to strontianite ($SrCO_3$) (Fig. 6d, ML-557-4c). These two minerals, strontianite and celestite are often found in association, together with barite, calcite and sulphur [28].

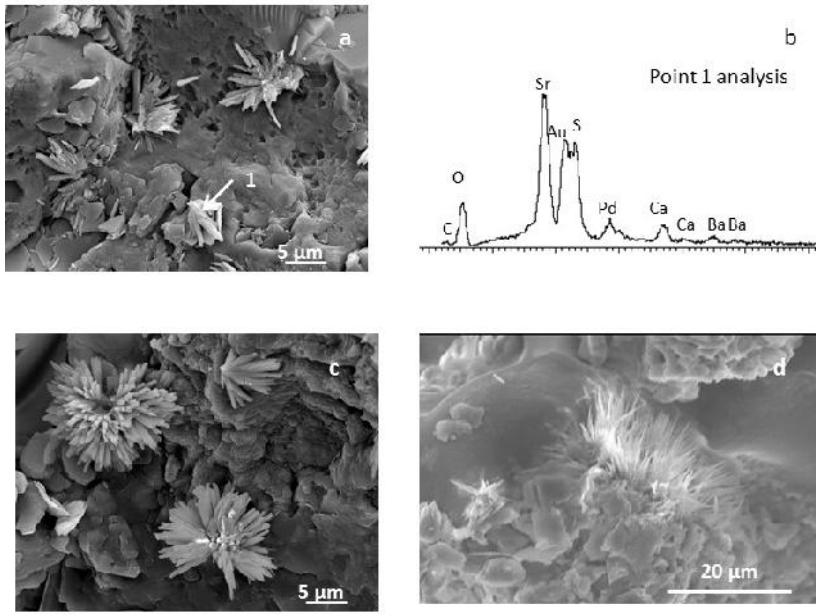

Fig. 6. FESEM images of calcite (Ca) and radiating crystal of celestite (Ce) grown on the calcite porosity (a – c); EDS spectrum (b) of the selected site – point 1 on celestite (see arrow) (a); SEM image of acicular crystals of strontianite (d).

Halite appears with cubic habit showing high crystalline character (Fig. 7a, ML-557-4a) or in malformed cubes. Well-formed cubic crystals reflects low evaporation rate [29, 30].

Dissolution features are observed from halite: one showing many grains with well rounded edges (Fig. 7b, ML-557-3), and another one forming an amorphous thin film with small corroded portions (Fig. 7c). EDS analysis (Fig. 7d) confirms the presence of halite by Na and Cl composition. This one is associated to typical elements from clay minerals (Al and Si). Indeed a large variety of crystal shapes observed in SEM, from massive and waxy forms to thin wickers, are reported in literature [29, 31, 32]. The type of crystal depends on several factors, such as the evaporation rate and the substrate characteristics [29, 30, 33]. The crystallisation conditions of halite are fairly well defined [29, 30, 33].

Kaolinite is the dominant clay mineral present in the studied samples (Tables 2 and 3). It occurs in two main ranges of morphological varieties: books (book-shaped parallel intergrowths) (Fig. 8a) and vermicular aggregates (Fig. 8b). The kaolinite vermiforms (accordion-like) have a length of ~13µm and are ~5µm across. Smectite crystals occur as platelets tending to form very thin films with a veil-like texture, or thin aggregates with diffuse outlines. These platelets show a typical swelling-related feature [34], especially curled edges (Fig. 8c, e and f). EDS spectrum of smectite (Fig. 8d) yields the corresponding high peaks of Si and Al and the smaller one of Mg, K and Fe. Fig. 8c was collected on the coastline cliff sandstone (PBA sample), while the other ones (Fig. 8e and f) on the dinosaur footprints, in the Museum (ML-557-4b and ML-557-3 samples, respectively). These last two samples, previously selected under stereomicroscope, were observed under the blistered and laminated portions. These morphological features may be related with the presence of smectite and smectitic mixed-layers, and gypsum.

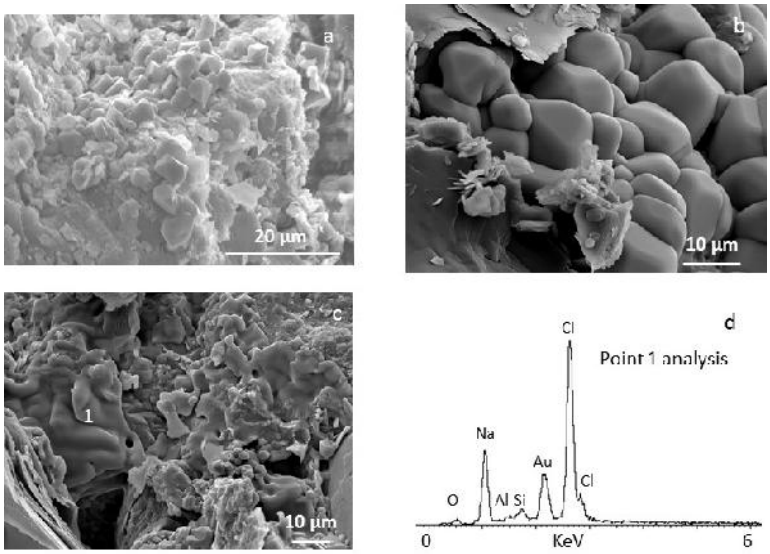

Fig. 7. SEM image of cubic crystals of halite (a), and FESEM images of halite grains with rounded edges (b); amorphous thin film with corroded edges (c); EDS spectrum (d) of the selected site on the amorphous film – point 1 (c).

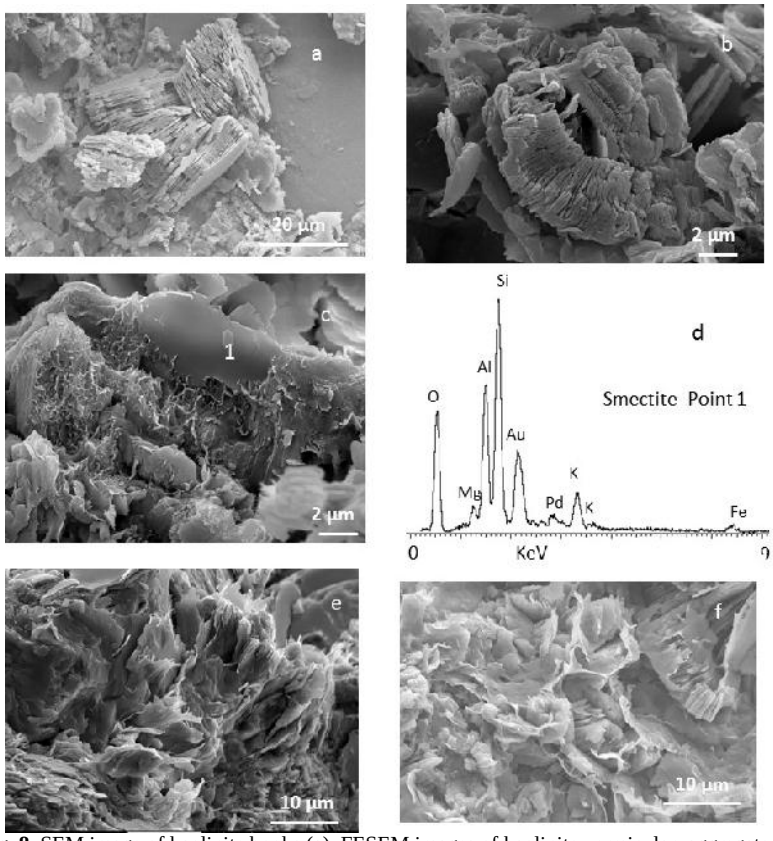

Fig. 8. SEM image of kaolinite books (a), FESEM images of kaolinite vermicular aggregates (b) and different textural features of smectite (c-e-f); EDS spectrum (d) of the selected site on the smectite – point 1(c).

E. Sebástian et al. [35], when studied the decay mechanism of the sandstone used in the construction of the Church of San Mateo in Tarifa (Cádiz, Spain) also identified interstratified chlorite-smectite clays among the minerals that make up the rock. These authors considered the main decay mechanism of the stone applied in that monument the swelling (or expansion) and shrinking of the clay minerals that form the cement or the matrix of that sandstone. The layer structure of the clay minerals makes them susceptible to retain moisture between layers. Nevertheless the swelling behaviour in stone materials depends on the type and amount of clay minerals present, their surface charges the cations in the double layer [36].

Smectite in the presence of water may undergo intracrystalline swelling. Indeed the morphological aspect of smectite identified in the dinosaur footprints, namely the curled edges, is a typical swelling-related feature.

Moreover if the pores in the rock contain an electrolyte in solution, clay minerals may also be subjected to osmotic-type swelling processes [37, 38, 39] enhancing thus the swelling potential of that stones. According to K.E. Schmittner and P. Giresse [40] sodium chloride is one of the most effective electrolytes in osmotic swelling of clays. In this study halite was identified by XRD in the bulk rock and also visualized by FESEM.

Water-soluble salts

Water-soluble salts in the dinosaur footprints were analysed. As shown in Figurer 9a, ion chromatography reveals the dominance of chlorides, with must lower levels of sulphates and nitrates (almost non-existent). In fact, the XRD and FESEM analysis shows that halite (NaCl) is one of the minerals that characterize the mineralogical composition of the studied sites (Table 2, Fig. 7). Nevertheless gypsum ($CaSO_4 \cdot 2H_2O$) (Table 2) and celestite ($SrSO_4$) (Table 2, Fig. 6a and c) were also identified.

Electrical conductivity measurements (Fig. 9b) are in agreement with the anions concentrations of the water-soluble fraction. Moreover the presence of salts increased the pH values from 5.73 (a slightly acidic pH value due to the low ion content in deionised water) to almost neutral values (7.59 - 7.92).

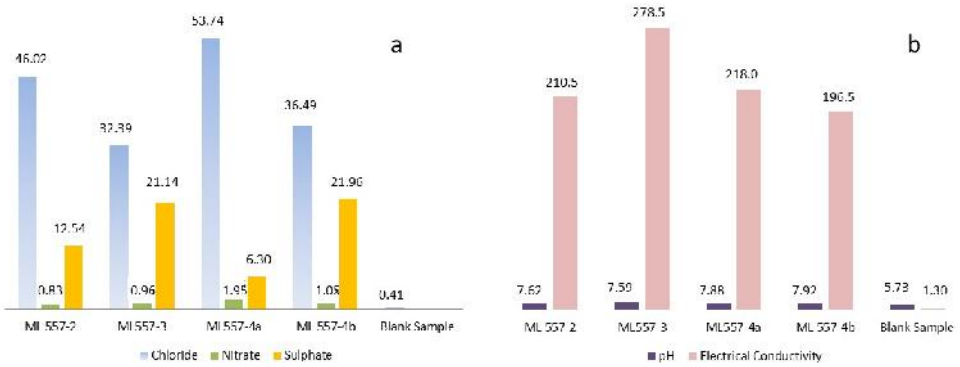

Fig. 9. Water-soluble salts in the dinosaur footprints:
(a) anions concentration (mg.L-1) and (b) electrical conductivity ($\mu S.cm^{-1}$) and pH.

The salts present in the footprints are neutral salts (pH values comprised between 6-8), as confirmed by the XRD analysis where halite is clearly the dominant salt (even with low concentrations). So, no alkaline soluble salts (i.e. pH > 8) were detected and thus several saline sources are then eliminated such as alkaline building materials (or restoration/conservation materials), such as cement, hydraulic lime or water glass [41, 42].

Chlorides are extremely dangerous salts because they are very soluble and hygroscopic. Once on solution they are very mobile and thus they penetrate and break-up many crystalline

structures [43]. Authors such as E.M. Winkler and P.L. Singer [44], R.J. Flatt [45] and M. Steiger [46] found that sodium chloride causes crystallization pressures much higher than for example the one that happens with sodium sulphate-mirabilite (between 2 and 7 times higher), although it is widely admitted that mirabilite causes more damage than sodium chloride [29, 47].

High concentrations of chlorides detected in the studied samples of the footprints are mainly related to the geographical localization were they were found, i.e., on a coastline cliff. Indeed the behavior of stone materials close to the sea is conditioned by an environment in which the principal negative parameter coincides with the presence of marine aerosol [48]. The damage due to sea-salt appears both as efflorescences, when the migration of the salts to the surface of the stone is faster than the rate of drying, and as powdering and crumbling when the migration is slower than the dry rate and the solute crystallizes within the pores and cracks at varying depths in the stone [48]. In fact one of the main deterioration patterns identified in the dinosaur footprints was powdering.

Past conservation treatments

Infrared spectra displayed a complementary information to the XRD analyses, namely in what concerns the characterization of past conservation treatments. In fact, in archaeological and paleontological works various organic polymers have been used, as consolidants and adhesives functions [49]. The principal aims of this application at the preparation procedures (fields works or laboratory) are to preserve the morphologic structure and to give more stability and durability in the field work, transportation, museum collection or deposit [49, 50].

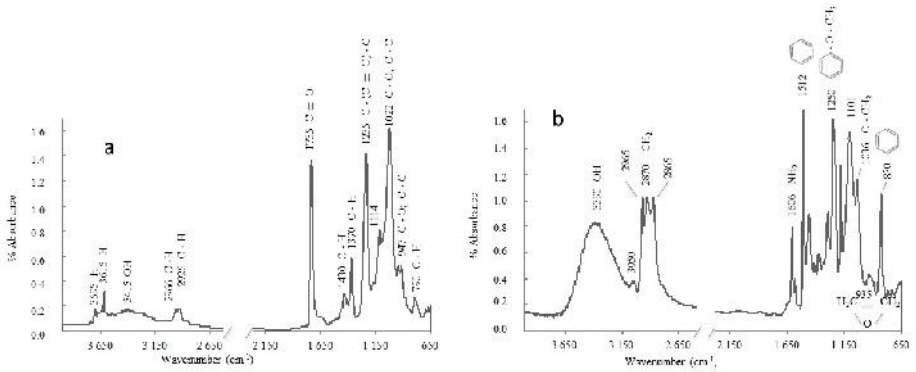

Fig. 10. µFTIR spectra of material composing the peeling (a) and of the material composing the film (b).

The spectra obtained from the material that composes the peeling (Fig. 3g and Fig. 10a) are characterized by several sharp and intense peaks: a dominant band at 1735cm^{-1} can be assigned to a –C=O stretching vibration associated to acetate groups, complemented by two less intense peaks at 1430cm^{-1} and 1370cm^{-1}, an asymmetric and symmetric bending vibration, respectively, associated to –C-H bending. A peak at 1235 cm^{-1} can be related to the asymmetric stretching of –C–(C=O)–C of ester groups. A double peak with a maximum intense at 1022cm^{-1} and other the lower intense at 947cm^{-1} can also assigned to C-O and C-C stretching. There is also a doublet with less intense peacks, associated with the –CH3 and –CH2 antisymmetric stretching vibration at 2966cm^{-1} and 2926cm^{-1}. Other less intense pecks at 790, 696 and 652cm^{-1} associated to C-H rocking vibration were identified. Therefore it seems that a poly(vinyl) acetate [51-56] was applied in the past laboratory treatments prior to exhibition. According to J.S. Johnson [49] poly(vinyl) acetate resins are commonly used in the paleontological/archaeological conservation field as consolidants and found to have good long-

term stability. Nevertheless these resins can become soft and sticky in warm temperatures [49]. Other problems mentioned when using with poly(vinyl) acetate emulsions include large particle size, acid pH (3.0 - 6.0), high viscosity, low glass transition temperature, and high moisture absorption properties [49].

In what concerns the material composing the film observed in the central part of the finger of the ML557-3 footprint (Fig. 4d), the FTIR analysis (Fig. 10b) show that an epoxy resin was applied as an adhesive. In fact this spectrum presents similarities to those presented by E.G. Karayannidou et al. [57], S.-C. Chen et al. [58] and M. Sánchez-Soto et al. [59]. It presents a less intense peak at 935cm^{-1} that corresponds to an oxirane ring. The absorption band at 3390cm^{-1} is related of the hydroxyl group. The three intense pecks at 2965, 2870, 2865cm^{-1} are stretching vibration of the $–CH_2–$ groups. There are an absorption peak at 1606cm^{-1}, associated at a stretching vibrations of the primary amino group ($-NH_2$). The peaks at 1512cm^{-1} and 830cm^{-1}, are possibly are associated to p-phenylene groups. The ether group is identified by three absorption peaks at 1250, 1101 and 1036cm^{-1}. The former peak (1036cm^{-1}) is related to the aliphatic carbon-oxygen stretching ($-O–CH_2-$) and the other intense peak, 1250cm^{-1} is result of the aromatic carbon-oxygen stretching.

Epoxy resins are used because of their strong adhesive force, having attained adhesive strength of up to 30 MPa [60]. This property makes these products appropriate for glueing broken pieces together. In fact a significant facture occurred in the ML557-3 (Fig. 4b) and it was necessary to solve it. Nevertheless this material presents nowadays yellowing and according to A. Davidson and S. Alderson [61] yellowing is generally considered a sign of degradation and may be indicative of other changes in the material over time.

Environment thermohygrometric conditions

The environment in which collections are stored is assumed by the scientific community as an important element to ensure the long-term safety and preservation of the collections. Collections as those presented in this study can be very sensitive to fluctuations in air temperature and relative humidity.

The most relevant thermohygrometric characteristics of indoor environmental conditions of the Museum as well as Lourinhã outdoor conditions are presented in Fig. 11 and Table 4. During the monitoring period, i.e., eight months, indoor temperature and relative humidity were comprised between 8.8°C and 22.5°C and 48.8% and 87.6%, respectively (Table 4). Outdoor temperature and relative humidity were comprised between 7.0°C and 27.6°C and 54.0% and 100%, respectively (Table 4).

Table 4. Daily thermohigrometric parameters measured outdoor and indoor

		Temperature (°C)		**Relative Humidity (%)**	
		Outdoor	*Indoor*	*Outdoor*	*Indoor*
From 2. November 2013 to 6. March 2014	Average	12.2	14.0	82.0	71.6
	Standard Deviation	2.2	1.6	9.9	10.7
	Minimum	7.0	8.8	54.0	48.8
	Maximum	17.7	18.0	97.0	87.6
From 24.May 2013 to 29. September 2014	Average	18.9	20.8	82.5	75.3
	Standard Deviation	2.4	1.1	7.1	4.2
	Minimum	12.8	18.5	61.0	59.1
	Maximum	27.6	22.5	100.0	82.5

Air temperature and relative humidity near the dinosaur footprints follow the outdoor climate (Fig. 11). However slightly higher daily temperatures (average daily difference 2.2°C) and lower daily relative humidities were registered indoors (average daily difference 9.1%). Only significant average daily relative humidity differences occur between indoor and outdoor

environments (according to the t-test performed). The thick walls of the building reduce the effect of short term outdoor relative humidity variations.

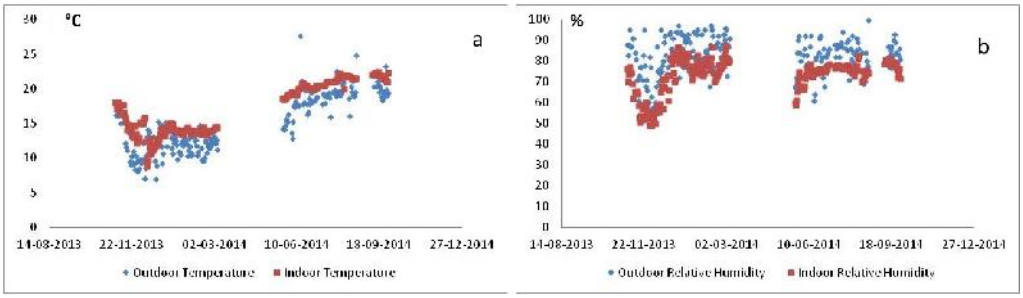

Fig. 11. Average daily values of outdoor temperature and indoor temperature (a) and of outdoor relative humidity and indoor relative humidity (b).

Non-stable, mainly, hygrometric conditions inside the Museum will favor periodical crystallization or solubilization of salts. Analyzing all data concerning indoor relative humidity one can affirm that 52.8% of the mean daily values are higher than 75%. According to C. Price and P. Brimblecombe [62] the common case of sodium chloride in association with calcium sulfate, as those identified in the present study, can cause severe damage wherever the relative humidity fluctuates within the range 75-100%. Therefore several authors [62, 63, 64] recommended that an object must be kept in a controlled environment at a humidity below the critical RH equilibrium point of the salts in the object. Nevertheless fluctuations below 75% RH, as those registered in 47.2% of the mean daily values in Lourinhã Museum, will also contribute to deterioration of these specimens in the long-term. Indeed S. Nunberg and A.E. Charola [65] verified that relatively minor fluctuations in relative humidity, even at ranges, well below the equilibrium relative humidity of the salt or salt mixtures, can cause damage to the salt-contaminated ceramic bodies. However the observed damage was lesser and occurred at a much slower rate than when the materials were left at a relative humidity equal to or above the equilibrium relative humidity even if this humidity was maintained constant.

So, the indoor environment cannot be neglected when analyzing the dinosaur footprint's causes of decay.

Conclusions

Extent and severe decay processes are in progress in three Late Jurassic sandstone dinosaur footprints exhibited in museum environment. The deterioration patterns observed are the result of a combined action of the intrinsic properties of the stone material and also of external agents of decay. In what concerns the environmental conditions two different aspects must be mentioned: (i) the exposure to the marine spray that these dinosaur footprints were submitted prior to their removal to a museum environment, and therefore high concentrations of chlorides were detected and (ii) the microclimate conditions in the museum, namely significant oscillations in air relative humidity favor periodical crystallization or solubilization of salts. The mineralogical composition of the sandstone where these footprints were preserved also determines to a large extent its behavior and vulnerability against physical or chemical aggressions, mainly through the presence of swelling clay minerals (smectite and chlorite-

smectite mixed-layer). Moreover past conservation interventions must also be mentioned as potential elements contributing to the present severe decay exhibited by the dinosaur footprints. Indeed a poly(vinyl) acetate resin was identified and conducted to the detachment of the stone material from the dinosaur footprint surfaces.

Based on the evaluation of the causes and mechanisms involved in the dinosaur footprint decay, some conservation measures needs to be undertaken, namely through stabilization of thermohygrometric indoor conditions, some form of consolidation may also be necessary to restore some strength to the dinosaur footprints. Moreover salt reduction from the sandstone surfaces is also advisable.

Acknowledgments

The authors thank to Museu da Lourinhã for their continued support and the use of its facilities. Special thanks to Carla Tomás for her suggestions and help with preparation of drawings. We acknowledge Jesper Milàn (GeoCenter Faxe, Denmark) that found the tracks, helped collecting and providing photos.

FCT is acknowledged for the Project UID/ECI/04028/2013 to CERENA and Project UID/GEO/04683/2013 to ICT.

References

[1] M.G. Lockley, D.D. Gillete, *Dinosaur tracks and traces: an overview*, **Dinosaur Tracks and Traces** (Editors: D.D. Gillette and M.G. Lockley),, Cambridge University Press, Cambridge, 1989, pp. 3-10.

[2] W.A.S. Sarjeant, *Ten paleoichnological commandments: A standardized procedure for the description of fossil vertebrate footprints*, **Dinosaur Tracks and Traces** (Editors: D.D. Gillette and M.G. Lockley), Cambridge University Press, Cambridge, 1989, pp. 369-370.

[3] R.E. Reynolds, *Dinosaur Trackways in the Lower Jurassic Aztec Sandstone of California*, **Dinosaur Tracks and Traces** (Editors: D.D. Gillette and M.G. Lockley), Cambridge University Press, Cambridge, 1989, pp. 285-292.

[4] P.J. Currie, *Dinosaur tracksites of Western Canada*, **Dinosaur Tracks and Traces** (Editors: D.D. Gillette and M.G. Lockley), Cambridge University Press, Cambridge, 1989, pp. 293-300.

[5] R.A. Thulborn, M. Wade, *A footprint as a history of movement*, **Dinosaur Tracks and Traces** (Editors: D.D. Gillette and M.G. Lockley), Cambridge University Press, Cambridge, 1989, pp. 51-56.

[6] N. Agnew, H. Griffin, M. Wade, T. Tebble, W. Oxnam, *Strategies and techniques for the preservation of fossil tracksites: an Australian example*, **Dinosaur Tracks and Traces** (Editors: D.D. Gillette and M.G. Lockley), Cambridge University Press, Cambridge, 1989, pp. 397-407.

[7] S.Y. Shelton, *Conservation of vertebrate paleontology collections*, **Vertebrate Paleontological Techniques**, **1**, 1994, pp. 3-33.

[8] S.Y. Shelton, D.S. Chaney, *An evaluation of adhesives and consolidants recommended for fossil vertebrates*, **Vertebrate Paleontological Techniques**, **1**, 1994, pp. 35-45.

[9] C. Bisulca, L.K. Elkin, A. Davidson, *Consolidation of Fragile Fossil Bone From Ukhaa Tolgod, Mongolia (Late Cretaceous) With Conservare OH100*, **Journal of the American Institute for Conservation**, **48**(1), 2009, pp. 37-50.

[10] J.L. Down, E. Kaminska, *A preliminary study of the degradation of cyanoacrylate adhesives in the presence and absence of fossil*, **Journal of Vertebrate Paleontology**, **26**(3), 2006, pp. 519-525.

[11] N.H. Agnew, W.B. Oxnam, *Conservation of the Lark Quarry dinosaur trackway*, **Curator: The Museum Journal**, **26**(3), 1983, pp. 219-233.

[12] S.J. Lee, N.R. Chim, I.S. Choi, *Study on the influence of the clay minerals to the conservation for shale stone with dinosaur's footprint*, **Advanced Materials Research** (Original title: 신소재연구), 24, 2012, pp. 92-96

[13] S.Y. Shelton, R.C. Barnett, M.D. Magruder, *Conservation of a dinosaur trackway exhibit*, **Collection**, **9**(1), 1993, pp. 17-26.

[14] S. Leal, O. Mateus, C. Tomas, A. Dionísio, *Degradation processes and consolidation of Late Jurassic sandstone dinosaur tracks in museum environment (Museum of Lourinhã, Portugal)*, **Proceedings of EGU General Assembly Conference Abstracts**, 16, 27 April – 02 May 2014, Vienna, Austria, 2014, p. 9026.

[15] G. Hill, *The sedimentology and lithostratigraphy of the Upper Jurassic Lourinhã formation, Lusitanian Basin, Portugal*, **Ph.D.Thesis**, The Open University, Milton Keynes, UK, 1988, 292 p.

[16] R.R. Leinfelder, R.C.L. Wilson, *Third-order sequences in an Upper Jurassic rift-related second-order sequence, central Lusitanian Basin, Portugal*, **Mesozoic and Cenozoic Sequence Stratigraphy of European Basins** (Editors: P.C. de Graciansky, J. Hardenbol, T. Jacquin and P.R. Vail), SEPM Spec. Publ., 60, 1998, pp. 505–525.

[17] T. Myers, N.J. Tabor, L.L. Jacobs, O. Mateus, *Palaeoclimate of the Late Jurassic of Portugal: comparison with the Western United States*, **Sedimentology**, **59**, 2012, pp.1695–1717.

[18] * * *, **Illustrated Glossary on Stone Deterioration Patterns**, Champigny/Marne, ICOMOS International Scientific Committee for Stone (ISCS), 2008.

[19] J. Delgado Rodrigues, *Defining, mapping and assessing deterioration patterns in stone conservation projects*, **Journal of Cultural Heritage**, **16**(3), 2015, pp. 267–275.

[20] H. Siedel, S. Siegesmund, *Characterization of stone deterioration in buildings*, **Stone in Architecture** (Editors: S. Siegesmund and R. Snethlage), Springer-Verlag Berlin Heidelberg, 2011, pp. 347-410.

[21] D.M. Moore, R.C. Reynolds**, X-ray Diffraction and the Identification and Analysis of Clay Minerals**, Oxford University Press, New York, 1997.

[22] P. Larqué, F. Weber, *Techniques de Préparation des Minéraux Argileux en Vue de l'analyse par Diffraction des Rayons-X*, **Notes Techniques de l'Institut de Géologie,** Université de Strasbourg, 1978, pp. 1-33.

[23] A. Dionísio, M.A. Sequeira Braga, J.C. Waerenborgh, *Clay minerals and iron oxides-oxyhydroxides as fingerprints of firing effects in a limestone monument*, **Applied Clay Science**, **42**(3-4), 2009, pp. 629-638.

[24] T. Valente, P. Gomes, M.A. Sequeira Braga, A. Dionísio, J. Pamplona, J.A. Grande, *Iron and arsenic-rich nanoprecipitates associated with clay minerals in sulfide-rich waste dumps*, **Catena**, **131**, 2015, pp. 1–13.

[25] B.J. Smith, A.V. Turkington, P.A. Warke, P.A. M., J.J. Basheer McAlister, J. Meneely, J.M. Curran, *Modelling the rapid retreat of building sandstones: a case study from a polluted maritime environment*, **Natural Stone, Weathering Phenomena, Conservation Strategies and Case Studies** (Geological Society, London, Special Publications), **205** 2002, pp. 347-362.

[26] A.V. Turkington, T.R. Paradise, *Sandstone weathering: A century of research and innovation*, **Geomorphology**, **67**, 2005, pp. 229–253.

[27] G. W. Brindley, G. Brown, **Crystal Structures of Clay Minerals and Their X-Ray Identification**, Monograph No. 5, Mineralogical Society, London, 1980.

[28] C. Klein, C.S. Hurlbut, **Manual of Mineralogy, After J.D. Dana,** 20th Edition, John Wiley & Sons, New York, 1985.

[29] C. Rodriguez-Navarro, E. Doehne, *Salt weathering: Influence of evaporation rate, supersaturation and crystallization pattern*, **Earth Surface Processes and Landforms**, **24**, 1999, pp. 191-209.

[30] M. Gomez-Heras, R. Fort, *Patterns of halite (NaCl) crystallization in building stone conditioned by laboratory heating regimes*, **Environmental Geology**, **52**(2), 2007, pp. 259–267.

[31] H. Eswaran, G. Stoops, A. Abathi, *SEM morphology of halite (NaCl) in soil*, **Journal of Microscopy**, **120**, 1980, pp. 343-352.

[32] C. Rodriguez-Navarro, L. Linares-Fernandez, E. Doehne, E. Sebastian, *Effects of ferrocyanide ions on NaCl crystallization in porous stone*, **Journal of Crystal Growth**, **243**(2-4), 2002, pp. 503-516.

[33] N. Shahidzadeh-Bonn, S. Rafaï, D. Bonn, G. Wegdam, *Salt crystallization during evaporation: impact of interfacial properties*, **Langmuir**, **24**(16), 2008, pp. 8599– 8605.

[34] K.-H. Henning, **Electron Micrographs (TEM, SEM) of Clays and Clay Minerals**, Schriftenreihe für Geologische Wissenschaften. Series in Geological Science, Heft 25, Akademie – Verlag Berlin, 1986,

[35] E. Sebastián, G. Cultrone, D. Benavente, L. Linares Fernandez, K. Elert, C. Rodriguez-Navarro, *Swelling damage in clay-rich sandstones used in the church of San Mateo in Tarifa (Spain)*, **Journal of Cultural Heritage**, **9**, 2008, pp. 66-76.

[36] F.T. Madsen, M. Müller-Vonmoos, *The swelling behaviour of clays*, **Applied Clay Science**, **4**, 1989, pp. 143-156.

[37] R. Snethlage, E. Wendler, *Moisture cycles and sandstone degradation*, **Saving Our Architectural Heritage: The Conservation of Historic Stone Structures** (Editors: N.S. Baer and R. Snethlage), John Wiley & Sons, Chichester and New York, 1996, pp. 7–24.

[38] C. Rodriguez-Navarro, E. Hansen, E. Sebastián, W.S. Ginell, *The role of clays in the decay of ancient Egyptian limestone sculptures*, **Journal of the American Institute for Conservation**, **36**, 1997, pp. 151-163.

[39] G. Scherer, I. Jiménez-González, *Swelling clays and salt crystallization: The damage mechanisms and the role of consolidants*, **Proceedings of the International Symposium in Stone Consolidation in Cultural Heritage: Research and Practice**, 6-7 May, 2008, Lisbon, Portugal, 2008, pp. 29–40.

[40] K.E. Schmittner, P. Giresse, *The impact of atmospheric sodium on erodibility of clay in a coastal Mediterranean region*, **Environmental Geology**, **37**, 1999, pp. 195-206.

[41] R.J. Schaffer, **The weathering of natural building stones**, Special Report nº 18, Building Research Establishment, Garston, 1932.

[42] A. Arnold, K. Zehnder, *Crystallization and habits of salt efflorescences on walls II. Conditions of crystallization*, **Proceedings of the Fifth International Congress on the Deterioration and Conservation of Stone**, 25-27 September 1985, Lausanne, Switzerland, 1985, pp. 269–277.

[43] G.G. Amoroso, V. Fassina, **Stone Decay and Conservation - Atmospheric Pollution, Cleaning, Consolidation and Protection**, Elsevier, Amsterdam, 1983.

[44] E.M. Winkler, P.C. Singer, *Crystallization of salt in stone and concrete*, **Geological Society of America Bulletin**, **83**, 1972, pp. 3509-3514.

[45] R.J. Flatt, *Salt damage in porous materials: how high supersaturations are generated*, **Journal of Crystal Growth**, **242,** 2002, pp. 435-454.

[46] M. Steiger, *Crystal growth in porous materials—I: the crystallization pressure of large crystals*, **Journal of Crystal Growth**, **282**, 2005, pp. 455–469.

[47] A.S. Goudie, H.A. Viles, **Salt Weathering Hazard**, JohnWiley & Sons, Chichester, 1997.

[48] F. Zezza, *Inland dispersion of marine spray and its effects on monument stone*, **Proceedings of the 5th International Symposium, Conservation of Monuments in the Mediterranean Basin**, 5-8 April 2000, Sevilla, Spain, 2000, pp. 23-42.

[49] J.S. Johnson, *Consolidation of Archaeological Bone: A Conservation Perspective*, **Journal of Field Archaeology**, **21**(2), 1994, pp. 221-233.

[50] L. López-Polín, *Possible interferences of some conservation treatments with subsequent studies on fossil bones: A conservator's overview*, **Quaternary International**, **275**, 2012, pp. 120-127.

[51] J.L. Ferreira, M.J. Melo, A.M. Ramos, *Poly(vinyl acetate) paints in work of art: A photochemical approach. Part 1*, **Polymer Degradation and Stability**, **95**, 2010, pp. 453-461.

[52] M.T. Doménech-Carbó, M.F. Silva, E. Aura-Castro, L. Fister-López, S. Kröner, M.L. Martínez-Bazán, X. Má-Barberá, M.F. Mecklenburg, L. Osete-Cortina, A. Doménech, J.V. Gimeno-Adelantado, D.J. Yusá-Marco, *Study of behaviour on simulated daylight ageing of artist' acrylic and poly(vinyl acetate) paint films*, **Analytical and Bioanalytical Chemistry**, **399**, 2011, pp. 2921-2937.

[53] I.S. Elashmawi, N.A. Hakeem, E.M. Abdelrazek, *Spectroscopic and thermal studies of PS/PVAc blends*, **Physics B**, **403**, 2008, pp. 3547-3552.

[54] S. Wei, V. Pintus, M. Schreiner, *Photochemical degradation study of polyvinyl acetate paints used in artworks by Py-GC/MS*, **Journal of Analytical and Applied Pyrolysis**, **97**, 2012, pp. 158-163.

[55] F. Toja, D. Saviello, A. Nevin, D. Comelli, M. Lazzari, G. Valentini, L. Toniolo, *The degradation of poly(vinyl acetate) as a material for design objects: A multi-analytical study of the effect of dibutyl phthalate plasticizer. Part 1*, **Polymer Degradation and Stability, 97**, 2012, pp. 2441-2448.

[56] D. Chelazzi, A. Chevalier, G. Pizzorusso, R. Giorgi, M. Menu, P. Baglioni, *Characterization and degradation of poly(vinyl acetate)-based adhesives for canvas paintings*, **Polymer Degradation and Stability, 107**, 2014, pp. 314-320.

[57] E.G. Karayannidou, D.S. Achilias, I.D. Sideridou, *Cure kinetics of epoxy-amine resins used in the restoration of works of art from glass or ceramic*, **European Polymer Journal**, **42**, 2006, pp. 3311-3323.

[58] S-C. Chen, H-T. Chiu, C-P. Ye, *Study of Ionic Polymer Toughening Epoxy Resin*, **Journal of Applied Polymer Science**, **86**, 2002, pp. 3740-3751.

[59] M. Sánchez-Soto, P. Pagés, T. Lacorte, K. Briceño, F. Carracco, *Curing FTIR study and mechanical characterization of glass bead filled trifunctional epoxy composites*, **Composites Science and Technology**, **67**, 2006, pp. 1974-1985.

[60] R. Snethlage, *Stone conservation*, **Stone in Architecture** (Editors: S. Siegesmund and R. Snethlage), Springer-Verlag, Berlin Heidelberg, 2011, pp. 411-544.

[61] A. Davidson, S. Alderson, *An introduction to solution and reaction adhesives for fossil preparation*, **Proceedings of the First Annual Fossil Preparation and Collections Symposium**, April 2009, Petrified Forest National Park, USA, 2009, pp. 53-62.

[62] C. Price, P. Brimblecombe, *Preventing salt damage in porous materials*, **Proceedings of Preventive Conservation: Practice, Theory and Research**, 12-16 September 1994, Ottawa, Canada, 1994, pp. 90-93.

[63] D. Erhardt, M. Mecklenburg, *Relative humidity re-examined*, **Proceedings of Preventive Conservation: Practice, Theory and Research**, 12-16 September 1994, Ottawa, Canada, 1994, pp. 32-38.

[64] M. Steiger, A. Zenert, *Crystallization properties of salt mixtures: comparison of experimental results and model calculations*, **Proceedings of 8th International Congress on Deterioration and Conservation of Stone,** 30 September - 4 October 1996, Berlin, Germany, 1996, pp. 90-93.

[65] S. Nunberg, A.E. Charola, *Salts in ceramic bodies II: Deterioration due to minimal changes in relative humidity*, **Internationale Zeitschrift für Bainstandsetzen und Baudenkmalpflege, 7**(2), 2001, pp. 131-146.

Received: February, 10, 2016
Accepted: September, 03, 2016